
Improving Long Handwritten Text Line Recognition with Convolutional Multi-way Associative Memory

Duc Nguyen

Cinnamon AI Lab, Vietnam
john@cinnamon.is

Nhan Tran

Cinnamon AI Lab, Vietnam
lucas@cinnamon.is

Hung Le

Deakin University, Australia
lethai@deakin.edu.au

Abstract

Convolutional Recurrent Neural Networks (CRNNs) excel at scene text recognition. Unfortunately, they are likely to suffer from vanishing/exploding gradient problems when processing long text images, which are commonly found in scanned documents. This poses a major challenge to goal of completely solving Optical Character Recognition (OCR) problem. Inspired by recently proposed memory-augmented neural networks (MANNs) for long-term sequential modeling, we present a new architecture dubbed Convolutional Multi-way Associative Memory (CMAM) to tackle the limitation of current CRNNs. By leveraging recent memory accessing mechanisms in MANNs, our architecture demonstrates superior performance against other CRNN counterparts in three real-world long text OCR datasets.

1 Introduction

Since first introduced, CRNN for Handwritten Text Recognition (HTR) has been constantly breaking state-of-the-art results [8, 31, 39], and being deployed in industrial applications [5, 6]. The gist of CRNN involves a convolutional feature extractor that encodes visual details into latent vectors, followed by a recurrent sequence decoder that turns the latent vectors into human-understandable characters. The whole architecture is trained end-to-end via Connectionist Temporal Classification (CTC) loss function [11] or attention mechanism [1, 19, 21].

Inside CRNN, the role of the sequence decoder (often implemented as Long Short-Term Memory [18]) has been reported to serve as a language model [33]. In [33], the authors observe that a learned OCR model attains higher accuracy for meaningful text line than for random text line. Experimental results from [38] also support this claim, in that an OCR model performs worse when tested on languages other than the language it is trained on (see Fig. 1). These results intuitively make sense because the knowledge of surrounding characters can provide clues to ascertain correct prediction. We hypothesize that this effect is even more pronouncing for HTR, where handwriting style variations and real world conditions can render characters visually confusing and unrecognizable, making predictions of such characters only feasible by referring to the surrounding context. As a result, enhancing the sequence decoder would improve CRNN performance.

Despite the promising empirical results, the LSTM as well as other RNN-based models is incapable of remembering long context due to vanishing/exploding gradient problems [3, 26, 30]. Current HTR datasets, which contain only scene text or short segments of texts are not challenging enough to expose the weakness. However, when approaching industrial data, which often involve transcription of the whole line of documents written in complicated languages, RNN-based decoders may fail to achieve good results.

Recently, a new class of neural network architecture, called Memory-Augmented Neural Network (MANN), has demonstrated potentials to replace RNN-based methods in sequential modeling. In essence, MANNs are recurrent controller networks equipped with external memory modules, in

Text-line Image	<i>Und bist du kühn und hälst du Stich,</i>
English	<i>Lind bist du kühn und häilst du Stich,</i>
German	<i>Und bist du kühn und häilst du Stich,</i>
French	<i>Lund bist du kühn und häilst du Stich,</i>
Mixed-data	<i>Und bist du kühn und häilst du Stich,</i>

Figure 1: Models trained on English, German, French, Mix-of-3 give prediction on a German text line (taken from [38])

which the controllers can interact with external memory unit via attention mechanisms [14]. Compared to LSTM, instead of storing hidden states in a single vector of memory cells, a MANN can store and retrieve its hidden states in multiple memory slots, making it more robust against exploding/vanishing gradient problem. MANNs have been experimented to perform superior to LSTM in language modeling tasks [16, 22] and thus beneficial to HTR where language modelling supports recognition. However, for this problem, to the best of our knowledge, there is no work currently employing MANN.

In this work, we adapt recent memory-augmented neural networks by integrating an external memory module into a convolutional neural network. The CNN layers read the input image, encoding it to a sequence of visual features. At each timestep of the sequence, two controllers will be used to store the features into the memory, access the memory in multiple refinement steps and generate an output. The output will be passed to a CTC layer to produce the CTC loss and the final predicted character. In summary, our main contributions are:

1. We introduce a memory-augmented recurrent convolutional architecture for OCR, called Convolutional Multi-way Associative Memory (CMAM),
2. We demonstrate the new architecture’s performance on 3 handwritten datasets: English IAM, Chinese SCUT-EPT and a private Japanese dataset.

2 Related Work

2.1 Convolutional Recurrent Neural Networks

Attempts to improve CRNN have mostly been focused on the convolutional encoder. Starting with the vanilla implementation [36], convolution layers have since been incorporated with gating mechanism [5], recurrent connections [40, 27], residual connections [6, 10, 43], and used alongside with dropout [31, 32], or Maxout [17]. Multi-Dimensional LSTM (MDLSTM) [12], which is often used in the feature encoder, can also serve as the sequence decoder [13, 31, 39]. On the other hand, improvement on the sequence decoder has received little attention. [37] proposes GMU, inspired by the architectures of both LSTM and GRU [7], and achieves good results on both online English and Chinese handwriting recognition tasks. [8] controls the shape of gating functions in LSTM with learnable scales. Recently, there are some attempts that replace CTC with Seq2Seq decoder, both without [34] and with attention mechanism [4] support for decoding. Hybrid models between CTC and attention decoder [19, 21] are also proposed and gain big improvement in Chinese and Japanese speech recognition.

2.2 Memory-augmented Neural Networks

Memory-augmented neural networks (MANN) have emerged as a new promising research topic in deep learning. In MANN, the interaction between the controller and the memory is differentiable, allowing it to be trained end-to-end with other components in the neural network [14, 41]. Compared to LSTM, it has been shown to generalize better on sequences longer than those seen during training [14, 15]. This improvement comes at the expense of more computational cost. However, recent advancements in memory addressing mechanisms allow MANN to perform much more efficiently [26]. For practical applications, MANNs have been applied to many problems such as meta

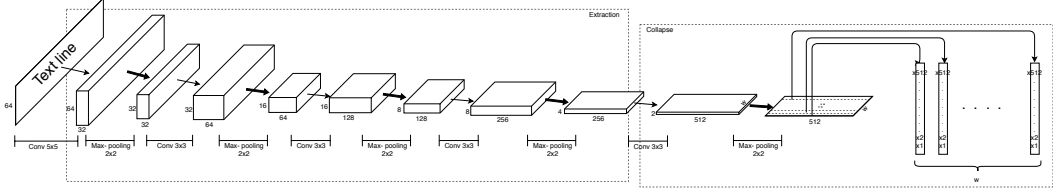


Figure 2: Convolutional layers

learning [35], healthcare [24, 25], dialog system [23], process analytic [20] and extensively in question answering [29] and language modeling [16]. Our work (CMAM) is one of the first attempts to utilize MANN for HTR tasks.

3 Proposed System

3.1 Visual Feature Extraction with Convolutional Neural Networks

In our CMAM, the component of convolutional layers is constructed by stacking the convolutional and max-pooling layers as in a standard CNN model. Such component is used to extract a sequential feature representation from an input image. Before being fed into the network, all the images need to be scaled to the same height. Then a sequence of feature vectors is extracted from the feature maps produced by the component of convolutional layers, which is the input for the memory module. Specifically, each feature vector of a feature sequence is generated from left to right on the feature maps column by column. This means the i -th feature vector is the concatenation of the i -th columns of all the maps (see Fig. 2). Each of the feature vector is then fed to a fully-connected layer to produce the final input x_t for the memory module.

3.2 Sequential Learning with Multi-way Associative Memory

In this section, we propose a new memory-augmented neural network, namely Multi-way Associative Memory (MAM) that is designed for HTR tasks.

3.2.1 Memory-augmented neural network overview

A memory-augmented neural network (MANN) consists of an LSTM controller, which frequently accesses and modifies an external memory $M \in \mathbb{R}^{N \times D}$, where N and D are the number of memory slots and the dimension of each slot, respectively. At each time step, the controller receives a concatenation of the input signal x_t and the previous read values r_{t-1} from the memory to update its hidden state and output as follows,

$$h_t, o_t = LSTM([x_t, r_{t-1}], h_{t-1}) \quad (1)$$

The controller output o_t then is used to compute the memory interface ξ_t and the short-term output y_t^s by applying linear transformation,

$$\xi_t = W_\xi o_t \quad (2)$$

$$y_t^s = W_s o_t \quad (3)$$

where W_ξ, W_s are trainable weight parameters. The interface ξ_t in our specific model is a set of vectors $\{k_t^{rj}, \beta_t^{rj}, f^{rj}, k_t^w, \beta_t^w, v_t, e_t, g_t^{alc}, g_t^w\}$ responsible for controlling the memory access, which includes memory reading and writing procedures (see 3.2.3 and 3.2.4, respectively). After the memory is accessed, the read values for current step r_t are computed and combine with the short-term output y_t^s , producing the final output of the memory module as the following,

$$y_t = W_y [y_t^s, r_t] \quad (4)$$

where W_y is trainable weight parameter. With the integration of read values, the final output y_t contains not only short-term information from the controller, but also long-term context from the memory. This design was first proposed in [14] and has become a standard generic memory architecture for sequential modeling [14, 15, 23, 24, 25].

3.2.2 Multi-way Associative Memory

We leverage the standard memory-augmented architecture by marrying bidirectional control with multi-hop memory accesses. In particular, we use two controllers: forward and backward controllers (both implemented as LSTM). The forward controller reads the inputs in forward order (from timestep 1-th to T -th) together with the read contents from the memory. It captures both short-term information from the past and long-term knowledge from the memory. On the other hand, the backward controller reads the inputs in backward order (from timestep T -th to 1-th) and thus only captures short-term information from the future. The backward controller maybe useful when the short-term future timesteps give local contribution to recognize the character at current timestep. However, it is unlikely that long-term future timesteps can have causal impact on current temporary output, which explains why the backward controller does not need to read content from the memory.

Moreover, our architecture supports multi-step computations to refine the outputs from the controllers (r_t and y_t^s) before producing the final output for that timestep. Let us denote L as the number of refinement steps. At l -th refinement step, the short-term output of previous refinement $y_{t,l-1}^s$ will be used as the input for the controllers. In particular, the controllers will compute their hidden states and temporary outputs for this refinement as follows,

$$h_{t,l}^f, o_{t,l}^f = LSTM^f \left([y_{t,l-1}^s, r_{t-1,l}], h_{t-1,l}^f \right), t = 1, \dots, T \quad (5)$$

$$h_{t,l}^b, o_{t,l}^b = LSTM^b \left(y_{t,l-1}^s, h_{t+1}^b \right), t = T, \dots, 1 \quad (6)$$

where $y_{t,-1}^s = x_t$. At timestep t -th, the forward controller updates its hidden state $h_{t,l}^f$ and compute temporary output $o_{t,l}^f$. The temporary output is stored in a buffer, waiting for the backward controller's temporary output $o_{t,l}^b$. The two buffered outputs are used to compute the memory interface vector $\xi_{t,l}$ and the short-term output $y_{t,l}^s$ as the following,

$$\xi_{t,l} = W_\xi \left[o_{t,l}^f, o_{t,l}^b \right] \quad (7)$$

$$y_{t,l}^s = W_s \left[o_{t,l}^f, o_{t,l}^b \right] \quad (8)$$

The refinement process simulates human multi-step reasoning. We often refer to our memory many times before making final decision. At each step of refinement, the controllers re-access the memory to get information representing the current stage of thinking. The representation is richer than the raw representation stored in the memory before refinement. For example, without refinement, at timestep t -th, the forward controller can only read values $r_{t,0}$ containing information from the past. However, from the first refinement step ($l \geq 1$), the memory is already filled with the information of the whole sequence, and thus a new refined read at timestep t -th can contain (very far if necessary) future information $r_{t,l}$. Fig. 3 illustrates the flow of operations in the architecture.

After refinement process, the final output y_t is computed by the generation unit as follows,

$$y_t = W_y \left[y_{t,L}^s, r_{t,L} \right] \quad (9)$$

We summarize the operation of MAM in Alg. 1. The algorithm can be considered as a generalization of the bidirectional control memory design proposed in [9].

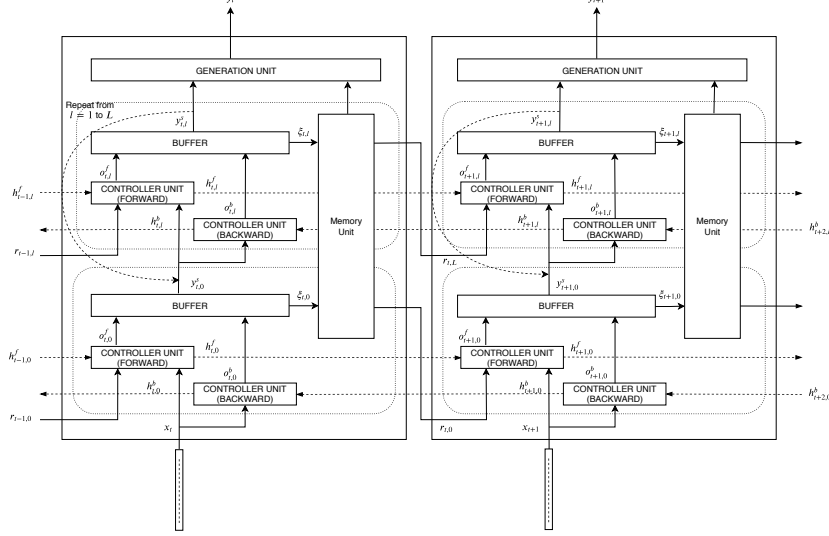


Figure 3: Multi-way Associative Memory Module. At each timestep, the two controllers collect information from the recent past and future, together with long-term values from the memory to make predictions. The memory is accessed in both horizontal and vertical ways (hence the name multi-way).

3.2.3 Memory reading

In our MAM, memory reading is inspired by content-based attention mechanism presented in [14, 15]. Let R be the number of reading heads, the read keys $k_t^{rj} \in \mathbb{R}^D, j = \overline{1, R}$ will be used for locating the j -th read-out. The addressing mechanism is mostly based on cosine similarity measure,

$$D(M_t(i), k_t^{rj}) = \frac{k_t^{rj} \cdot M_t(i)}{\|k_t^{rj}\| \cdot \|M_t(i)\|} \quad (10)$$

which is used to produce a content-based read-weight $w_t^{rj} \in \mathbb{R}^N$ whose elements are computed according to softmax function over memory's locations,

$$w_t^{rj}(i) = \text{softmax}(D(M_t(i), k_t^{rj}) \beta_t^{rj}) \quad (11)$$

Here, β_t^{rj} is the strength parameter. After the read weights are determined. the j -th read value r_t^j is retrieved as the following,

$$r_t^j = \sum_{j=1}^R w_t^{rj}(i) M_t(i) \quad (12)$$

The final read-out is the concatenation of all read values $r_t = [r_t^1, r_t^2, \dots, r_t^R]$.

Different from [15], we exclude temporal linkage reading mechanism from our memory reading. Recent analyses in [9] reveal that this mechanism increases the computation time and physical storage dramatically. By examining the memory usages, [9] also indicated that the temporal linkage reading are barely used in realistic tasks and thus could be safely removed without hurting the performance much. We follow this practice and only keep the content-based reading mechanism. We realize that the key-value based retrieval resembles traditional associative memory system [2]. The mechanism is critical for OCR tasks where reference to previous exposures of some visual feature may consolidate the confidence of judging current ones. When compared to recurrent networks in current OCR systems, which only use single visual feature stored in the hidden state to make prediction on the output, multiple visual features reference may provide the model with richer information and thus give better predictions.

Algorithm 1 Multi-way Memory Access Algorithm

Require: Given initial $r_{0,l}, h_{0,0}^f, h_{T+1,0}^b$, forward LSTM cell $LSTM^f$, backward LSTM cell $LSTM^b$, memory functions $read()$, $write()$ and input sequence $[x_1, x_2, \dots, x_T]$

1: Set $[y_{1,-1}^s, y_{2,-1}^s, \dots, y_{T,-1}^s] = [x_1, x_2, \dots, x_T]$

2: **for** $l = 0, L$ **do** $\triangleright L$ is the number of refinement steps

3: **for** $t = T, 1$ **do** $\triangleright T$ is the number of timesteps

4: $o_{t,l}^b, h_{t,l}^b = LSTM^b([y_{t,l-1}^s, h_{t+1,l}^b])$

5: **end for**

6: **for** $t = 1, T$ **do**

7: $o_{t,l}^f, h_{t,l}^f = LSTM^f([y_{t,l-1}^s, r_{t-1}], h_{t-1,l}^f)$

8: $\xi_{t,l} = W_\xi [o_{t,l}^f, o_{t,l}^b]$

9: $y_{t,l}^s = W_s [o_{t,l}^f, o_{t,l}^b]$

10: $write(\xi_{t,l})$

11: $r_{t,l} = read(\xi_{t,l})$

12: **end for**

13: **end for**

3.2.4 Memory writing

To build writing mechanism for our memory, we apply three different writing strategies. First, we make use of the dynamic memory allocation in [15]. This strategy tends to write to least-used memory slots. Let use the memory retention vector $\psi_t \in [0, 1]^N$ to determine how much each memory location will not be freed as follows,

$$\psi_t = \prod_{j=1}^R \left(1 - f_t^j w_{t-1}^{rj} \right) \quad (13)$$

where for each read head j , $f_t^j \in [0, 1]$ denotes the free gate emitted by the interface and w_{t-1}^{rj} denotes the read weighting vector from the previous timestep. The usage over N memory locations at current time-step t is given by $u_t \in [0, 1]^N$, which is called memory usage vector,

$$u_t = (u_{t-1} + w_{t-1}^w - u_{t-1} \circ w_{t-1}^w) \circ \psi_t \quad (14)$$

Then, the allocation vector is defined as the following,

$$a_t [\Phi_t [k]] = (1 - u_t [\Phi_t [k]]) \prod_{i=1}^{k-1} u_t [\Phi_t [i]] \quad (15)$$

in which, Φ_t contains elements from u_t in sorted order.

The second strategy we propose is the last-read writing, in which the location to be written is the previous read location. We define the previous read locations by averaging the previous read weights,

$$l_t = \frac{1}{R} \sum_{j=1}^R w_{t-1}^{rj} \quad (16)$$

By writing to the previous read address, we assume that after read, the content in that address is no longer important for future prediction. This assumption makes sense in OCR setting where some visual features only take part in recognizing one character. After the model refers to these visual features to make predictions, it is safe to remove them from the memory to save spaces for other important features.

The third strategy is the common content-based writing, which is similar to content-based reading. A content-based write weight is computed as follows,

$$c_t^w (i) = \text{softmax} (D (M_t (i), k_t^w) \beta_t^w) \quad (17)$$

Dataset	Language	#Writers	#Lines		Avg. characters per line	#Classes
			Train+valid	Test		
IAM	English	400	7,458	2,915	45.72	80
SCUT-EPT	Chinese	2986	40,000	10,000	26.41	4,058
Private	Japanese	N/A	14,594	2,940	49.83	2,227

Table 1: Characteristics of the datasets used in our experiments.

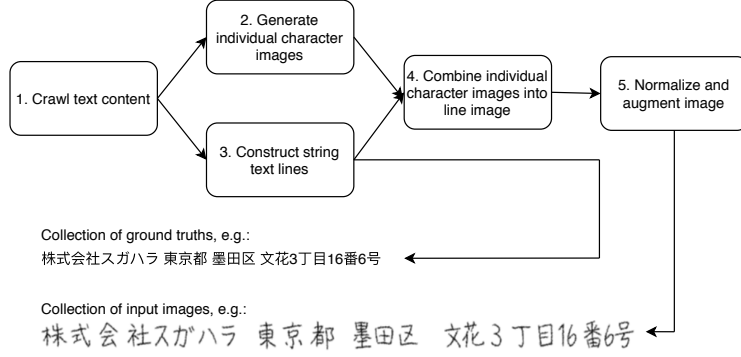


Figure 4: Synthetic Line Image Generation

where k_t^w and β_t^w are the key and strength parameters for content-based writing, respectively.

To allow the model to select amongst strategies and have the ability to refuse writing, a write mode indicator $g_t^{alc} \in \mathbb{R}^3$ and a write gate $g_t^w \in \mathbb{R}$ are used to compute the final write weight as the following,

$$w_t^w = g_t^w [g_t^{alc}(0) a_t + g_t^{alc}(1) l_t + g_t^{alc}(2) c_t] \quad (18)$$

where the write mode indicator g_t^{alc} and the write gate g_t^w are normalized using softmax and sigmoid functions, respectively.

Finally, the write-weight can be used together with the update value $v_t \in \mathbb{R}^D$, and erase value $e_t \in [0, 1]^D$ to modify the memory content as follows,

$$M_t = M_{t-1} \circ (E - w_t^w e_t^\top) + w_t^w v_t^\top \quad (19)$$

where \circ is element-wise product.

4 Experimental Evaluation

4.1 Experimental Settings

Baselines. The main baseline used across experiments is the traditional CRNN with the same CNN architecture presented in 3.1, coupled with the bidirectional 1D LSTM layers as proposed in [32]. We use DNC [15] as the decoder for visual sequence to form another MANN baseline against our memory-based architecture. Finally, we also include other results reported from previous works for SCUT-EPT dataset

Datasets. To validate our proposed model, we select IAM [28] and SCUT-EPT [44], which are two public datasets written in English and Chinese, respectively. We also collect a private dataset from our partner-a big corporation in Japan. This dataset is scanned documents written by Japanese scientists and thus, contains noises, special symbols, and more characters per line than the other datasets. The statistics of the three datasets are summarized in Table 1.

Since our aim is to recognize long text line by end-to-end models, we do not segment the line into words. Rather, we train the models with the whole line and report Character Error Rate (CER),

Model	Valid	Test
CRNN (BiLSTM)	13.19 ± 0.24	13.72 ± 0.16
DNC	14.15 ± 0.47	14.61 ± 0.34
CMAM ($l = 0$)	12.99 ± 0.40	13.39 ± 0.15
CMAM ($l = 1$)	10.72 ± 0.23	11.12 ± 0.20

Table 2: Character Error Rate (CER) on IAM dataset

Correct Rate (CR) and Accuracy Rate (AR) [42]. To fit with Chinese and Japanese datasets where there is no white-space between words, we exclude white-space from the vocabulary set and do not measure word error rate metrics.

4.2 Synthetically generated handwritten line images

This section describes the synthetic data generation process used for our experiments. We execute 5 steps as illustrated in Fig. 4. Specifically, we start by crawling some text contents, typically from news site or from Wikipedia, and remove bad symbols and characters from the text corpus (1). Since the corpus might contain unknown characters to us, i.e. characters that we do not have any visual knowledge. We obtain these characters (a) by scouting them on the web and (b) by generating them from fonts and apply random variations to make it less print-like and more handwriting-like (2). The corpus also largely contains text of paragraph level, so we break it down into text lines, each of which contains on average 15 characters (3). For each text line, we combine random individual character images to make line images (4). Finally, we normalize the line images to ease the abrupt variations produced by different image characters and we augment the line images to increase style variations. After this process, we have a collection of line images with their corresponding ground truth labels.

There are two purposes of using synthetic data. First, we generate data for tuning our implemented models (CRNN, DNC, CMAM). In particular, after training with 10,000 synthesized line images (both Latin and Japanese) on various range of hyper-parameters, we realize that the optimal memory size for MANN models is 16×16 with 4 read heads. The LSTM controller’s hidden sizes for DNC and CMAM are 256 and 196, respectively. For the CRNN baseline, the best configuration is 2-layer bidirectional LSTM of size 256. The optimal optimizer is RMSprob with a learning rate of 10^{-4} . Second, since collecting and labeling line images are labor-intensive, we increase the number of training images with synthetic data for the Japanese recognition task. We generate 100,000 Japanese line images to pre-train our models before fine-tuning them on the private Japanese dataset.

4.3 Latin Recognition Task

In this task, we compare our model with CRNN and DNC. Two variants of our CMAM are tested: one uses no refinement ($l = 0$) and the other uses one step of refinement ($l = 1$), respectively. This experiment is a simple ablation study to determine good configuration of CMAM for other tasks. We run each model 5 times and calculate the mean and standard deviation on CER metric. The final result is reported in Table 2.

Compared to other baselines, DNC is the worst performer, which indicates a naive application of this generic model on OCR tasks seem inefficient. Both versions of CMAM outperform other baselines including the common CRNN architecture. Increasing the number of refinement steps helps CMAM outperform CRNN more than 2%. The improvement is not big since the IAM’s text line is short and clean. It should be noted that our results are not comparable to that reported in other works [32] as we train on the whole line and discard white-space prediction. We also do not use any language model, pre-processing and post-processing techniques.

4.4 Chinese Recognition Task

In this experiment, we run CRNN and CMAM ($l = 1$) on SCUT-EPT dataset. Table 3 shows the CR and AR measurements of our implemented models and other baselines from [44]. CRNNs are still strong baselines for this task as they reach much higher accuracies than attentional models.

Model	CR	AR
CRNN (LSTM)	78.60	75.37
Attention	69.83	64.78
Cascade Attention	54.09	48.98
CRNN (BiLSTM, ours)	81.47	74.33
CMAM ($l = 1$)	82.14	74.45

Table 3: Correct Rate (CR) and Accuracy Rate (AR) on raw SCUT-EPT dataset.

Model	Original data		Enriched data	
	valid	test	valid	test
CRNN (BiLSTM, ours)	32.84	27.00	24.83	11.62
CMAM ($l = 1$)	17.55	12.99	15.66	10.71

Table 4: Character Error Rate (CER) on Japanese dataset

Compared to CRNN [44], our proposal CMAM can demonstrate higher CR by more than 3%, yet lower AR by 0.92%. However, CMAM outperforms our CRNN implementation on the two metrics by 0.67% and 0.12%, respectively.

4.5 Japanese Recognition Task

The OCR model is trained on 2 sources of datasets: synthetically generated handwritten line images (see Sec. 4.2) and a private in-house collected Japanese dataset. The dataset contains more than 17,000 handwritten line images, which is divided into training and testing sets (see Table 1). We split 2000 images from the training set to form the validation set. These images are obtained from scanned notebooks, whose lines are meticulously located and labeled by our dedicated QA team. It contains various Japanese character types (Katakana, Kanji, Hiragana, alphabet, number, special characters and symbols) to make our model work on general use cases.

We have conducted 2 experiments with the Japanese dataset. In the first experiment, we train the models directly with the real-world training set and report CER on the validation and testing set in Table 4 (middle column). As seen from the results, CMAM outperforms CRNN significantly where the error rates reduce around 14% in both validation and testing sets. This demonstrates the advantage of using memory to capture distant visual features in case the line text is long and complicated.

In the second experiment, we first train the models on 100,000 synthetic lines of images. After the models converge on the synthetic data, we continue the training on the real-world data. The result is listed in the rightmost column of Table 4. With more training data, both models achieve better performance. More specifically, the improvement can be seen clearer in the case of CRNN, which implies pre-training may be more important for CRNN than CMAM. However, CMAM can still reach lower error rates than CRNN on the validation and test set (9% and 1%, respectively).

5 Conclusion

In this paper, we present a new architecture for handwritten text recognition that augments convolutional recurrent neural network with an external memory unit. The memory unit is inspired by recent memory-augmented neural networks, especially the Differentiable Neural Computer, with extensions for new writing strategy and multi-way memory access mechanisms. The whole architecture is proved efficient for handwritten text recognition through three experiments, in which our model demonstrates competitive or superior performance against other common baselines from the literature.

References

- [1] Dzmitry Bahdanau, Kyunghyun Cho, and Yoshua Bengio. Neural machine translation by jointly learning to align and translate. *Proceedings of the International Conference on Learning Representations*, 2015.
- [2] Bill Baird, Morris W Hirsch, and Frank Eeckman. A neural network associative memory for handwritten character recognition using multiple chua characters. *IEEE Transactions on Circuits and Systems II: Analog and Digital Signal Processing*, 40(10):667–674, 1993.
- [3] Yoshua Bengio, Patrice Simard, and Paolo Frasconi. Learning long-term dependencies with gradient descent is difficult. *IEEE transactions on neural networks*, 5(2):157–166, 1994.
- [4] Théodore Bluche, Jérôme Louradour, and Ronaldo Messina. Scan, attend and read: End-to-end handwritten paragraph recognition with md_lstm attention. In *2017 14th IAPR International Conference on Document Analysis and Recognition (ICDAR)*, volume 1, pages 1050–1055. IEEE, 2017.
- [5] Théodore Bluche and Ronaldo Messina. Gated convolutional recurrent neural networks for multilingual handwriting recognition. In *2017 14th IAPR International Conference on Document Analysis and Recognition (ICDAR)*, volume 1, pages 646–651. IEEE, 2017.
- [6] Fedor Borisuk, Albert Gordo, and Viswanath Sivakumar. Rosetta: Large scale system for text detection and recognition in images. In *Proceedings of the 24th ACM SIGKDD International Conference on Knowledge Discovery & Data Mining*, pages 71–79. ACM, 2018.
- [7] Junyoung Chung, Caglar Gulcehre, KyungHyun Cho, and Yoshua Bengio. Empirical evaluation of gated recurrent neural networks on sequence modeling. *arXiv preprint arXiv:1412.3555*, 2014.
- [8] Patrick Doetsch, Michal Kozielski, and Hermann Ney. Fast and robust training of recurrent neural networks for offline handwriting recognition. In *2014 14th International Conference on Frontiers in Handwriting Recognition*, pages 279–284. IEEE, 2014.
- [9] Jörg Franke, Jan Niehues, and Alex Waibel. Robust and scalable differentiable neural computer for question answering. In *Proceedings of the Workshop on Machine Reading for Question Answering*, pages 47–59. Association for Computational Linguistics, 2018.
- [10] Yunze Gao, Yingying Chen, Jinqiao Wang, and Hanqing Lu. Reading scene text with attention convolutional sequence modeling. *arXiv preprint arXiv:1709.04303*, 2017.
- [11] Alex Graves, Santiago Fernández, Faustino Gomez, and Jürgen Schmidhuber. Connectionist temporal classification: labelling unsegmented sequence data with recurrent neural networks. In *Proceedings of the 23rd international conference on Machine learning*, pages 369–376. ACM, 2006.
- [12] Alex Graves, Santiago Fernández, and Jürgen Schmidhuber. Multi-dimensional recurrent neural networks. In *International conference on artificial neural networks*, pages 549–558. Springer, 2007.
- [13] Alex Graves and Jürgen Schmidhuber. Offline handwriting recognition with multidimensional recurrent neural networks. In *Advances in neural information processing systems*, pages 545–552, 2009.
- [14] Alex Graves, Greg Wayne, and Ivo Danihelka. Neural turing machines. *arXiv preprint arXiv:1410.5401*, 2014.
- [15] Alex Graves, Greg Wayne, Malcolm Reynolds, Tim Harley, Ivo Danihelka, Agnieszka Grabska-Barwińska, Sergio Gómez Colmenarejo, Edward Grefenstette, Tiago Ramalho, John Agapiou, et al. Hybrid computing using a neural network with dynamic external memory. *Nature*, 538(7626):471–476, 2016.
- [16] Caglar Gulcehre, Sarath Chandar, and Yoshua Bengio. Memory augmented neural networks with wormhole connections. *arXiv preprint arXiv:1701.08718*, 2017.

[17] Pan He, Weilin Huang, Yu Qiao, Chen Change Loy, and Xiaoou Tang. Reading scene text in deep convolutional sequences. In *Thirtieth AAAI Conference on Artificial Intelligence*, 2016.

[18] Sepp Hochreiter and Jürgen Schmidhuber. Long short-term memory. *Neural computation*, 9(8):1735–1780, 1997.

[19] Takaaki Hori, Shinji Watanabe, Yu Zhang, and William Chan. Advances in joint ctc-attention based end-to-end speech recognition with a deep cnn encoder and rnn-lm. *arXiv preprint arXiv:1706.02737*, 2017.

[20] Asjad Khan, Hung Le, Kien Do, Truyen Tran, Aditya Ghose, Hoa Dam, and Renuka Sindhgatta. Memory-augmented neural networks for predictive process analytics. *arXiv preprint arXiv:1802.00938*, 2018.

[21] Suyoun Kim, Takaaki Hori, and Shinji Watanabe. Joint ctc-attention based end-to-end speech recognition using multi-task learning. In *2017 IEEE International Conference on Acoustics, Speech and Signal Processing (ICASSP)*, pages 4835–4839. IEEE, 2017.

[22] Ankit Kumar, Ozan Irsoy, Peter Ondruska, Mohit Iyyer, James Bradbury, Ishaan Gulrajani, Victor Zhong, Romain Paulus, and Richard Socher. Ask me anything: Dynamic memory networks for natural language processing. In *International Conference on Machine Learning*, pages 1378–1387, 2016.

[23] Hung Le, Truyen Tran, Thin Nguyen, and Svetha Venkatesh. Variational memory encoder-decoder. In *Advances in Neural Information Processing Systems*, pages 1515–1525, 2018.

[24] Hung Le, Truyen Tran, and Svetha Venkatesh. Dual control memory augmented neural networks for treatment recommendations. In *Advances in Knowledge Discovery and Data Mining*, pages 273–284, Cham, 2018. Springer International Publishing.

[25] Hung Le, Truyen Tran, and Svetha Venkatesh. Dual memory neural computer for asynchronous two-view sequential learning. In *Proceedings of the 24th ACM SIGKDD International Conference on Knowledge Discovery; Data Mining*, KDD ’18, pages 1637–1645, New York, NY, USA, 2018. ACM.

[26] Hung Le, Truyen Tran, and Svetha Venkatesh. Learning to remember more with less memorization. In *International Conference on Learning Representations*, 2019.

[27] Chen-Yu Lee and Simon Osindero. Recursive recurrent nets with attention modeling for ocr in the wild. In *Proceedings of the IEEE Conference on Computer Vision and Pattern Recognition*, pages 2231–2239, 2016.

[28] U-V Marti and Horst Bunke. The iam-database: an english sentence database for offline handwriting recognition. *International Journal on Document Analysis and Recognition*, 5(1):39–46, 2002.

[29] Alexander Miller, Adam Fisch, Jesse Dodge, Amir-Hossein Karimi, Antoine Bordes, and Jason Weston. Key-value memory networks for directly reading documents. *arXiv preprint arXiv:1606.03126*, 2016.

[30] Razvan Pascanu, Tomas Mikolov, and Yoshua Bengio. On the difficulty of training recurrent neural networks. In *International Conference on Machine Learning*, pages 1310–1318, 2013.

[31] Vu Pham, Théodore Bluche, Christopher Kermorvant, and Jérôme Louradour. Dropout improves recurrent neural networks for handwriting recognition. In *2014 14th international conference on frontiers in handwriting recognition*, pages 285–290. IEEE, 2014.

[32] Joan Puigcerver. Are multidimensional recurrent layers really necessary for handwritten text recognition? In *2017 14th IAPR International Conference on Document Analysis and Recognition (ICDAR)*, volume 1, pages 67–72. IEEE, 2017.

[33] Ekraam Sabir, Stephen Rawls, and Prem Natarajan. Implicit language model in lstm for ocr. In *2017 14th IAPR International Conference on Document Analysis and Recognition (ICDAR)*, volume 7, pages 27–31. IEEE, 2017.

- [34] Devendra Kumar Sahu and Mohak Sukhwani. Sequence to sequence learning for optical character recognition. *arXiv preprint arXiv:1511.04176*, 2015.
- [35] Adam Santoro, Sergey Bartunov, Matthew Botvinick, Daan Wierstra, and Timothy Lillicrap. Meta-learning with memory-augmented neural networks. In *International conference on machine learning*, pages 1842–1850, 2016.
- [36] Baoguang Shi, Xiang Bai, and Cong Yao. An end-to-end trainable neural network for image-based sequence recognition and its application to scene text recognition. *IEEE transactions on pattern analysis and machine intelligence*, 39(11):2298–2304, 2017.
- [37] Li Sun, Tonghua Su, Shengjie Zhou, and Lijun Yu. Gmu: A novel rnn neuron and its application to handwriting recognition. In *2017 14th IAPR International Conference on Document Analysis and Recognition (ICDAR)*, volume 1, pages 1062–1067. IEEE, 2017.
- [38] Adnan Ul-Hasan and Thomas M Breuel. Can we build language-independent ocr using lstm networks? In *Proceedings of the 4th International Workshop on Multilingual OCR*, page 9. ACM, 2013.
- [39] Paul Voigtlaender, Patrick Doetsch, and Hermann Ney. Handwriting recognition with large multidimensional long short-term memory recurrent neural networks. In *2016 15th International Conference on Frontiers in Handwriting Recognition (ICFHR)*, pages 228–233. IEEE, 2016.
- [40] Jianfeng Wang and Xiaolin Hu. Gated recurrent convolution neural network for ocr. In *Advances in Neural Information Processing Systems*, pages 335–344, 2017.
- [41] Jason Weston, Sumit Chopra, and Antoine Bordes. Memory networks. *arXiv preprint arXiv:1410.3916*, 2014.
- [42] Fei Yin, Qiu-Feng Wang, Xu-Yao Zhang, and Cheng-Lin Liu. Icdar 2013 chinese handwriting recognition competition. In *2013 12th International Conference on Document Analysis and Recognition*, pages 1464–1470. IEEE, 2013.
- [43] Hongjian Zhan, Qingqing Wang, and Yue Lu. Handwritten digit string recognition by combination of residual network and rnn-ctc. In *International Conference on Neural Information Processing*, pages 583–591. Springer, 2017.
- [44] Yuanzhi Zhu, Zecheng Xie, Lianwen Jin, Xiaoxue Chen, Yaoxiong Huang, and Ming Zhang. Scut-ept: New dataset and benchmark for offline chinese text recognition in examination paper. *IEEE Access*, 7:370–382, 2018.